ISME2010-2870

A class of shape memory alloy constitutive models based on a new set of internal variables

J. Arghavani[1], F. Auricchio[2,3,4], A. Reali[2,3] , S. Sohrabpour[1]

[1] Department of Mechanical Engineering, Sharif University of Technology, Tehran, Iran
[2] Dipartimento di Meccanica Strutturale, Università degli studi di Pavia, Pavia, Italy
[3] Istituto di Matematica Applicata e Tecnologie Informatiche del CNR, Pavia, Italy
[4] European Centre for Training and Research in Earthquake Engineering (EUCENTRE), Pavia, Italy

Abstract
In this paper we use the set of internal variables recently proposed by the authors to introduce a class of constitutive models for shape memory alloys. Such a class is based on the thermodynamics of irreversible processes with internal variables. A measure of martensite fraction and a measure of the preferred direction of variants are used as internal variables, describing thermo-elastic reversible martensitic phase transformation and stress-induced martensite reorientation, respectively. We identify some constitutive models available in the literature and show that they belong to the introduced class of models. Moreover, we compare three constitutive models with two sets of experimental data available in the literature.

Keywords: shape memory alloys, phase transformation, constitutive model, internal variables

Introduction

Intelligent, smart or functional materials exhibit special properties that make them a suitable choice for industrial applications in many branches of engineering. Among different types of smart materials, shape memory alloys (SMAs) have unique features known as pseudo-elasticity (or superelasticity), one-way and two-way shape memory effects [1,2]. Today, superelastic Nitinol is a common and well-known engineering material in the medical industry [3].

The origin of these material features is the reversible thermo-elastic martensitic phase transformation between a high symmetry, usually cubic, austenitic phase and a low symmetry martensitic phase. Austenite is a solid phase, usually characterized by a body-centered cubic crystallographic structure, which transforms to martensite by means of a lattice shearing mechanism. When the transformation is driven by the temperature, the shape changes in the variants compensate each other, resulting in no macroscopic deformation. However, in the case of a stress-induced martensitic transformation, a certain martensite variant, which is favorable to the applied stress, is formed preferentially, exhibiting a macroscopic shape change in the direction of the applied stress. Upon unloading or heating, this shape change disappears through the reversible motion of the martensite plates in the parent phase [1,4].

Selecting an appropriate set of internal variables as a macroscopic consequence of the micro-structural changes is one of the most important issues of phenomenological modeling [5,6]. Their introduction and definition would play a basic, crucial and even decisive role in arriving at a physically sound and pertinent constitutive formulation with a simple, consistent structure. As a result, their physical foundations should be placed under as stringent and thorough examination as possible. Since the internal variables are related to the micro-structural mechanisms, their evolution equations should be well established with relevant physical considerations [6].

To this end, in this study, the set of internal variables proposed in Arghavani et al. [7] is used to describe the behavior of shape memory alloys with an emphasis on reorientation. The amount of stress-induced martensite norm is chosen as a scalar internal variable to measure the amount of inelastic strain due to phase transformation while the average direction of different variants or preferred direction of variants is chosen as a tensorial internal variable to represent the inelastic strain direction. So, the physical origins of internal variables may be clearly interpreted as phase transformation and variant reorientation. In this way, transformation and reorientation can be described with more flexibility.

A class of three-dimensional constitutive models is derived to describe phase transformation and reorientation in shape memory alloys. To this end, in Section 2, we first define the Helmholtz free energy function and then derive the evolution equations satisfying the Clausius-Duhem inequality. We also discuss the definition of limit functions in a general case introducing in this way a class of models. In Section 3, we focus on particular members of the introduced class and identify them as models previously obtained in the literature. Section 4 is devoted to numerical tests and comparison of the models under different loading conditions; in particular the identified models are tested to reproduce non-proportional experiments available in the literature. Conclusions are finally drawn in Section 5.

A class of 3-D constitutive models for SMAs

According to Arghavani et al. [7], we select as internal variables a measure of the preferred direction of variants

along with the amount of martensite. Assuming small strains, we use the additive strain decomposition:

$$\boldsymbol{\varepsilon} = \boldsymbol{\varepsilon}^{e} + \boldsymbol{\varepsilon}^{ie} \tag{1}$$

where $\boldsymbol{\varepsilon}$, $\boldsymbol{\varepsilon}^{e}$ and $\boldsymbol{\varepsilon}^{ie}$ are the total, elastic and inelastic strain, respectively. We now introduce a scalar internal variable q defined as $q = \left\|\boldsymbol{\varepsilon}^{ie}\right\|$ and a tensorial internal variable $\mathbf{N}$ such that:

$$\boldsymbol{\varepsilon}^{ie} = q\mathbf{N} \tag{2}$$

Moreover, it is required that $0 \le q \le \varepsilon_L$ and $\left\|\mathbf{N}\right\| = 1$, where $\left\|\cdot\right\|$ is the usual Euclidean norm and ε_L is a material parameter corresponding to the maximum transformation strain reached at the end of the transformation during a uni-axial test.

The model assumes the total strain $\boldsymbol{\varepsilon}$ and the absolute temperature T as control variables, the norm of inelastic strain q and the average direction of martensite variants $\mathbf{N}$ as internal variables. Introducing the standard decomposition into volumetric and deviatoric part: $\boldsymbol{\varepsilon} = \frac{\theta}{3}\mathbf{1} + \mathbf{e}$, where $\theta = tr(\mathbf{e})$ and $\mathbf{e}$ is the deviatoric part of $\boldsymbol{\varepsilon}$, while $\mathbf{1}$ is the second-order identity tensor, the free energy density function Ψ for a polycrystalline SMA material is then expressed as the convex potential [7-11]:

$$\begin{aligned}\Psi(\theta,\mathbf{e},T,q,\mathbf{N}) = {} & \frac{1}{2}K\theta^2 + G\left\|\mathbf{e} - q\mathbf{N}\right\|^2 + \tau_M(T) \\ & + \frac{1}{2}hq^2 + I_{0,\varepsilon_L}(q) + \kappa(\left\|\mathbf{N}\right\| - 1)\end{aligned} \tag{3}$$

where K and G are respectively the bulk and the shear modulus, $\tau_M(T) = \beta\left\langle T - T_0\right\rangle$ with β a material parameter related to the dependency of the critical stress on the temperature, T_0 is the reference temperature and h defines the hardening of the phase transformation. Moreover, we make use of the indicator function

$$I_{0,\varepsilon_L}(q) = \begin{cases} 0 & if \;\; 0 \le q \le \varepsilon_L \\ +\infty & otherwise \end{cases} \tag{4}$$

in order to satisfy the inequality constraint on q. The Lagrange multiplier κ has been introduced to satisfy the equality constraint $\left\|\mathbf{N}\right\| = 1$. We have also made use of the positive part function $\left\langle\cdot\right\rangle$. Starting from the adopted free energy function Ψ and following standard arguments, we can derive the constitutive equations

$$\begin{cases} p = \dfrac{\partial\Psi}{\partial\theta} = K\theta \\ \mathbf{s} = \dfrac{\partial\Psi}{\partial\mathbf{e}} = 2G(\mathbf{e} - \mathbf{e}^{ie}) \\ \eta = -\dfrac{\partial\Psi}{\partial T} = -q\dfrac{\tau_M(T)}{\left|T - T_0\right|} \\ Q = -\dfrac{\partial\Psi}{\partial q} = \mathbf{s}:\mathbf{N} - (\tau_M(T) + hq + \gamma) \\ \mathbf{X} = -\dfrac{\partial\Psi}{\partial\mathbf{N}} = q\mathbf{s} - \kappa\mathbf{N} \\ K = -\dfrac{\partial\Psi}{\partial\kappa} = -\left\|\mathbf{N}\right\| + 1 = 0 \end{cases} \tag{5}$$

where

$$p = \frac{tr(\boldsymbol{\sigma})}{3}, \qquad \mathbf{s} = \boldsymbol{\sigma} - p\mathbf{1} \tag{6}$$

The quantities $\boldsymbol{\sigma}$, p, $\mathbf{s}$, η are respectively the Cauchy stress tensor, the volumetric or hydrostatic stress, the deviatoric part of the stress and the entropy. The thermodynamic stress-like quantities Q and $\mathbf{X}$ are associated to the internal variables q and $\mathbf{N}$. The variable γ results from the indicator function subdifferential $\partial I_{0,\varepsilon_L}(q)$ and it is defined as:

$$\partial I_{0,\varepsilon_L}(q) = \begin{cases} \gamma_1 \le 0 & if \;\; q = 0 \\ 0 & if \;\; 0 < q < \varepsilon_L \\ \gamma_2 \ge 0 & if \;\; q = \varepsilon_L \end{cases} \tag{7}$$

According to (5), the mechanical dissipation inequality reduces to

$$D^{mech} = \boldsymbol{\sigma}:\dot{\boldsymbol{\varepsilon}} - (\dot{\Psi} + \eta\dot{T}) = Q\dot{q} + \mathbf{X}:\dot{\mathbf{N}} \ge 0 \tag{8}$$

In order to satisfy the second law of thermodynamics and the mechanical dissipation inequality (8), we choose the following flow rules for internal variables:

$$\begin{cases} \dot{q} = \dot{\zeta}Q = \dot{\zeta}(\mathbf{s}:\mathbf{N} - (\tau_M + hq + \gamma)) \\ \dot{\mathbf{N}} = \dot{\lambda}\mathbf{X} = \dot{\lambda}(q\mathbf{s} - \kappa\mathbf{N}) \end{cases} \tag{9}$$

where $\dot{\zeta}$ and $\dot{\lambda}$ are non-negative consistency parameters. From equation $(5)_6$ we may conclude that $\mathbf{N}:\dot{\mathbf{N}} = 0$. Moreover double contracting both sides of equation $(9)_2$ with $\mathbf{N}$ and applying constraint, we can compute the Lagrange multiplier κ as $\kappa = q\mathbf{s}:\mathbf{N}$ and the thermodynamic force $\mathbf{X}$ reads as:

$$\mathbf{X} = q(\mathbf{s} - (\mathbf{s}:\mathbf{N})\mathbf{N}) = q\mathbf{Y} \tag{10}$$

where $\mathbf{Y} = \mathbf{s} - (\mathbf{s}:\mathbf{N})\mathbf{N}$ is the stress component normal to $\mathbf{N}$.

Now, we may redefine evolution equations as follows:

$$\begin{cases} \dot{q}\mathbf{N} = \dot{\zeta}Q\mathbf{N} = \dot{\zeta}(Q\mathbf{N} + k(q)\mathbf{Y}) \\ q\dot{\mathbf{N}} = \dot{\lambda}\mathbf{Y} \end{cases} \tag{11}$$

In order to describe phase transformation and reorientation evolution, we choose two limit functions F^{tr} and F^{re} defined as:

$$\begin{cases} F^{tr} = \left\| Q\mathbf{N} + k(q)\mathbf{Y} \right\| - R^{tr}(q) \\ F^{re} = \left\| \mathbf{Y} \right\| - R^{re}(q) \end{cases} \tag{12}$$

where $R^{tr}(q)$ represents the radius of the elastic domain and $R^{re}(q)$ controls the evolution direction of inelastic strain; in the expression of F^{tr}, the term $k(q)$ reflects the effect of reorientation on transformation. The limit function F^{re} affects reorientation by controlling the component of stress normal to the preferred direction of variants and the limit function F^{tr} affects transformation by controlling the transformation thermodynamic force components $Q\mathbf{N}$ in the preferred direction of variants, $\mathbf{N}$, and $k(q)\mathbf{Y}$ normal to that direction.

Also, for generality we can assume that transformation affects reorientation and define an interaction function $\bar{k}(q)$ which leads to redefined evolution equations as:

$$\begin{cases} \dot{q} = \dot{\zeta} Q \\ q\dot{\mathbf{N}} = \left(\dot{\lambda} + \bar{k}(q)\dot{\zeta} \right) \mathbf{Y} \end{cases} \tag{13}$$

We derived the evolution equations and the limit functions for a general case considering the effects of reorientation on transformation through $k(q)$ and using $\bar{k}(q)$ to account for the effects of transformation on reorientation. We now summarize the material law which defines a class of models as follows:

$$\begin{cases} p = K\theta \\ \mathbf{s} = 2G(\mathbf{e} - \mathbf{e}^{ie}) \\ Q = \mathbf{s} : \mathbf{N} - (\tau_M + hq + \gamma) \\ \mathbf{Y} = \mathbf{s} - (\mathbf{s} : \mathbf{N})\mathbf{N} \\ \dot{q} = \dot{\zeta} Q \\ q\dot{\mathbf{N}} = \left(\dot{\lambda} + \bar{k}(q)\dot{\zeta} \right) \mathbf{Y} \\ F^{tr} = \left\| Q\mathbf{N} + k(q)\mathbf{Y} \right\| - R^{tr}(q) \\ F^{re} = \left\| \mathbf{Y} \right\| - R^{re}(q) \\ \dot{\zeta} \geq 0, F^{tr} \leq 0, \dot{\zeta} F^{tr} = 0 \\ \left(\dot{\lambda} + \bar{k}(q)\dot{\zeta} \right) \geq 0, F^{re} \leq 0, \dot{\lambda} F^{re} = 0 \end{cases} \tag{14}$$

To decide on the form of interaction functions $k(q)$ and $\bar{k}(q)$ together with $R^{tr}(q)$ and $R^{re}(q)$, experimental observations should be considered.

Identification and comparison of some models belonging to the general class

Model 1. This model, elaborated by Auricchio and Petrini [9] from the original model of Souza et al. [11] is characterized by a simple reorientation mechanism and can be considered as a particular member of the introduced class of models, obtained for:

$$k(q) = 1, \quad \bar{k}(q) = 1, \quad R^{tr}(q) = R^{tr}, \quad R^{re}(q) \to +\infty \tag{15}$$

According to (15), we conclude that the limit function F^{re} is always negative which results in $\dot{\lambda} = 0$. In other words, in Model 1 this surface is never activated. Also this model considers the effect of reorientation on transformation $\left(k(q) \neq 0 \right)$ and since it is assumed that $\bar{k}(q) \neq 0$ reorientation is affected by transformation.

Model 2. This model, proposed by Panico and Brinson [12] and discussed by Arghavani [13], can be interpreted either as an extension of Model 1 (including a more flexible description of reorientation mechanism) or as a modification of the model presented by Panico and Brinson [12]. This model is also a particular member of the general class of models previously discussed, obtained for:

$$k(q) = 1, \quad \bar{k}(q) = 1, \quad R^{tr}(q) = R^{tr}, \quad R^{re}(q) = R^{re} \tag{16}$$

A saturation limit for the component of stress normal to the direction $\mathbf{N}$ is present, but similar to Model 1, orientation is affected by transformation $\left(\bar{k}(q) \neq 0 \right)$.

Model 3. This model, proposed by Arghavani et al, [7] is a member of the general class introduced before, but no effect on reorientation due to transformation is considered. The model is obtained for:

$$k(q) = 1, \quad \bar{k}(q) = 0, \quad R^{tr}(q) = R^{tr}, \quad R^{re}(q) = R^{re} \tag{17}$$

The evolution equations and limit functions for the three models are:

- *Model 1*

$$\begin{cases} \dot{q} = \dot{\zeta} Q \\ q\dot{\mathbf{N}} = \dot{\zeta} \mathbf{Y} \\ F^{tr} = \left\| Q\mathbf{N} + \mathbf{Y} \right\| - R^{tr} \end{cases} \tag{18}$$

- *Model 2*

$$\begin{cases} \dot{q} = \dot{\zeta} Q \\ q\dot{\mathbf{N}} = \left(\dot{\zeta} + \dot{\lambda} \right) \mathbf{Y} \\ F^{tr} = \left\| Q\mathbf{N} + \mathbf{Y} \right\| - R^{tr} \\ F^{re} = \left\| \mathbf{Y} \right\| - R^{re} \end{cases} \tag{19}$$

- *Model 3*

$$\begin{cases} \dot{q} = \dot{\zeta} Q \\ q\dot{\mathbf{N}} = \dot{\lambda}\mathbf{Y} \\ F^{tr} = \left\| Q\mathbf{N} + \mathbf{Y} \right\| - R^{tr} \\ F^{re} = \left\| \mathbf{Y} \right\| - R^{re} \end{cases} \tag{20}$$

The interesting point is that, all of the above mentioned differences appear only for non-proportional loading. In the case of proportional loading, $\mathbf{N} = \mathbf{s}/\|\mathbf{s}\|$, $\mathbf{Y} = \mathbf{0}$ and $\dot{\lambda} = 0$, so Models 1-3 as well as any other model of the proposed class reduce to:

$$\begin{cases} \dot{q} = \dot{\zeta} Q \\ F^{tr} = \left| Q \right| - R^{tr} \end{cases} \tag{21}$$

Models comparison with experimental data

In this section we perform several multiaxial non-proportional numerical tests to compare the three models identified in the previous Section. we also compare the models prediction and experimental data available in the literature. For this purpose we employ the tension-torsion experimental results from Sittner et al. [14], for which we identified the material parameters reported in Table 1.

Table 1 - Material parameters adopted for Sittner et al. [14] experiment

Parameter	Value	Unit
E	30700	MPa
ν	0.35	---
h	11000	MPa
ε_L	0.049	---
τ_M	150	MPa/K
T	285	K
R^{tr}	63.3	MPa

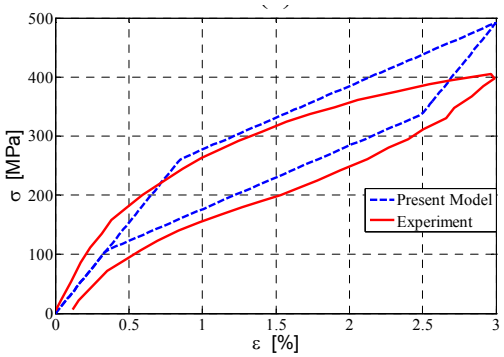

Figure 1. uniaxial tension behavior prediction by models and comparison with experimental results from [14]

Figure 1 shows the uniaxial behavior under a tension test. It is possible to see that models describe the behavior in a qualitative way.

Figure 2a shows a biaxial non-proportional path. At the first stage an axial stress of 240 MPa is applied and then the shear stress is increased to approximately 195 MPa at second stage, while the tension is kept constant. At stages 3 and 4, first tension and then shear loadings are sequentially unloaded, respectively. Comparison of models and experimental data is presented in Figure 2b. A qualitatively good agreement between experiments and simulations is observed for the case of model 3, in which the model is able to reproduce the main characteristics of the experimentally observed behavior. In particular model 3 can predict the coupling between axial and shear strains in a correct way at both stage 2 and 3.

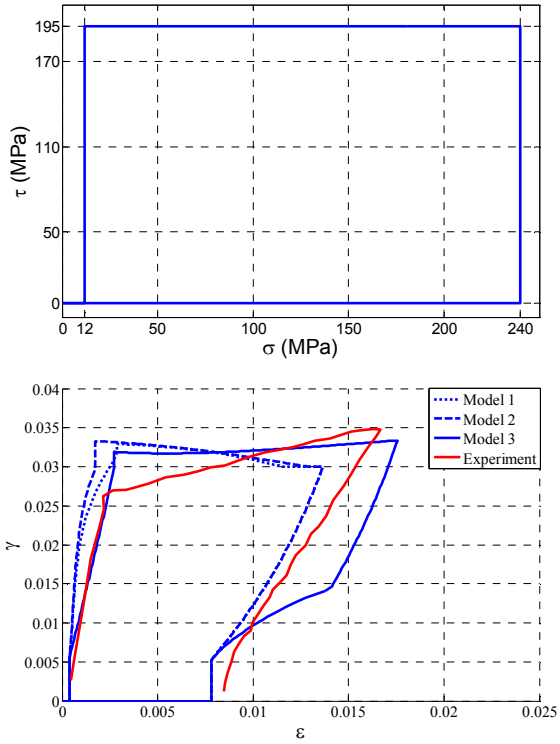

Figure 2. Comparison between models prediction and experimental [14] a) non-proportional biaxial tension-shear path b) comparison of predictions between model 1, 2 and 3 and experimental data.

Table 2- Material parameters adopted for Bouvet et al. [15,16] experiment

Parameter	Value	Unit
E	75000	MPa
ν	0.3	---
h	4233	MPa
ε_L	0.0585	---
τ_M	51	MPa/K
T	305	K
R^{tr}	16	MPa

We now consider the experimental data reported by Bouvet, et al. [15,16]. To this end, using experimental tension test data and some material parameters given in [16], material parameters are identified and reported in Table 2 and the realized behavior is compared with experimental data.

In Figure 3, we compare the models predictions with experimental data under uniaxial tension test.

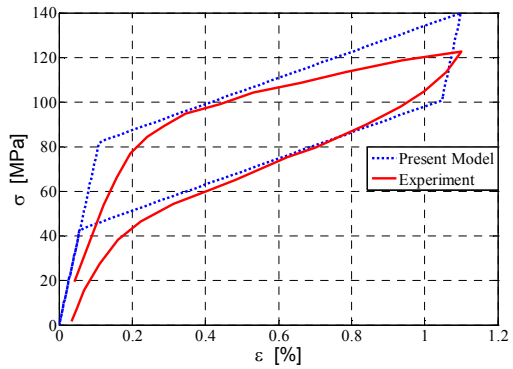

Figure 3. uniaxial tension behavior prediction by models and comparison with experimental results from [15]

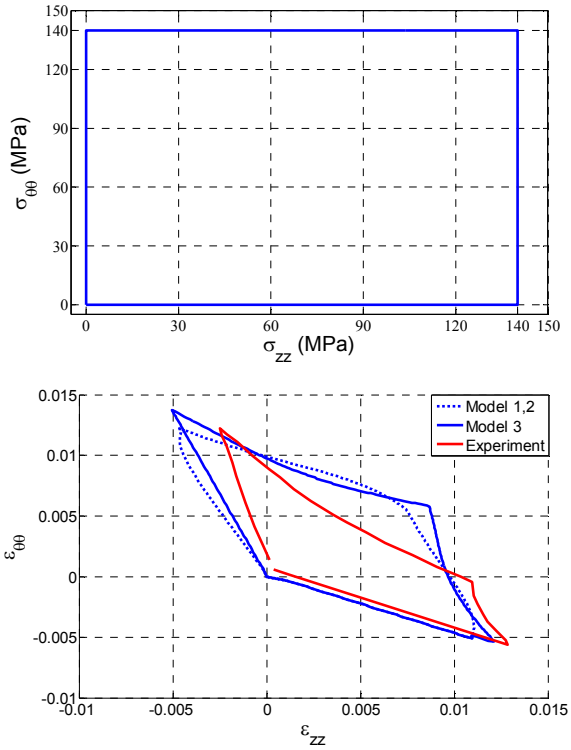

Figure 4. Simulation of the non-proportional biaxial loading a) loading path. b) comparison of models predictions and experimental data.

Figure 4 presents the simulation results under the biaxial non-proportional load (Figure 4a). As shown in Figure 4b, the identified models are in qualitatively good agreemrnt with experimental data.

According to the predictions by the models, it can be concluded that the proposed class of models presented in this paper can describe the reorientation phenomenon in SMAs under non-proportional loadings in a good qualitative way. The identified models need some improvements, such as considering the material parameter R^{re} as a function of q which is the subject of future work. With a physical and thermodynamical basis for describing reorientation mechanism, the proposed class of models can be improved to get an effective and simple tool to predict shape memory alloy-based structures, such as stents, implemented within a finite element program, constituting in this way a useful instrument for the design and analysis of SMA devices.

Identifying other members of the proposed class of models which can improve modeling capability by better describing the reorientation mechanism is a subject under investigation.

Conclusions

In this study we presented some new features of SMAs behavior modeling under non-proportional loading conditions. A recently proposed set of internal variables is used to propose a class of constitutive models; these variables are more physical and describe in a clear way phase transformation and reorientation. Based on new internal variables, a class of material models was proposed. Two interaction functions were introduced to capture the effect of phase transformation on variants reorientation and vice versa. It was shown that three previously proposed models can be considered as a particular case of the introduced general class of models. We also compared the three models under two different non-proportional loading conditions with available experimental data in the literature, while we showed that under proportional loadings, all models provide the same results.

References

[1] Otsuka, K., and Wayman, C. M., 1998. *Shape Memory Materials*. Cambridge University Press, Cambridge.

[2] Duerig, T. W., Melton, K. N., Stoekel, D., and Wayman, C. M., 1990. *Engineering Aspects of Shape Memory Alloys*. Butterworth-Heinemann, London.

[3] Duerig, T., Pelton, A., and Stöckel, D., 1999. An overview of nitinol medical applications. *Materials Science and Engineering A* 273-275**,** 149-160.

[4] Funakubo, H., 1987. *Shape Memory Alloys*. Gordon and Breach Science Publishers, New York.

[5] Fung, Y. C., 1994. *A first course in continuum mechanics*. Prentice Hall, Englewood Cliffs.

[6] Xiao, H., Bruhns, O., and Meyers, A., 2006. Elastoplasticity beyond small deformations. *Acta Mechanica* 182**,** 31-111.

[7] Arghavani, J., Auricchio, F., Naghdabadi, R., Reali, A., and Sohrabpour, S.,. A 3-D phenomenological constitutive model for shape memory alloys under multiaxial loadings, *International Journal of Plasticity* (in press)

[8] Auricchio, F., and Petrini, L., 2002. Improvements and algorithmical considerations on a recent three-dimensional model describing stress-induced solid phase transformations. *International Journal for Numerical Methods in Engineering* 55**,** 1255-1284.

[9] Auricchio, F., and Petrini, L., 2004a. A three-dimensional model describing stress-temperature induced solid phase transformations: solution algorithm and boundary value problems. *International Journal for Numerical Methods in Engineering* 61**,** 807-836.

[10] Auricchio, F., and Petrini, L., 2004b. A three-dimensional model describing stress-temperature induced solid phase transformations: thermomechanical coupling and hybrid composite applications. *International Journal for Numerical Methods in Engineering* 61**,** 716-737.

[11] Souza, A. C., Mamiya, E. N., and Zouain, N., 1998. Three-dimensional model for solids undergoing stress-induced phase transformations. *European Journal of Mechanics - A/Solids* 17**,** 789-806.

[12] Panico, M., and Brinson, L. C., 2007. A three-dimensional phenomenological model for martensite reorientation in shape memory alloys. *Journal of the Mechanics and Physics of Solids* 55**,** 2491-2511.

[13] Arghavani, J., in preparation. Thermomechanical behavior of shape memory alloys under nonproportional loading: Constitutive modelling and numerical inplementation in small and finite strains, *Ph.D. Thesis*, Sharif University of Technology, Iran.

[14] Sittner, P., Hara, Y., and Tokuda, M., 1995. Experimental study on the thermoelastic martensitic transformation in shape memory alloy polycrystal induced by combined external forces. *Metallurgical and Materials Transactions* A 26**,** 2923-2935.

[15] Bouvet, C., Calloch, S., and Lexcellent, C., 2002. Mechanical Behavior of a Cu-Al-Be Shape Memory Alloy Under Multiaxial Proportional and Nonproportional Loadings. *Journal of Engineering Materials and Technology* 124**,** 112-124.

[16] Bouvet, C., Calloch, S., and Lexcellent, C., 2004. A phenomenological model for pseudoelasticity of shape memory alloys under multiaxial proportional and nonproportional loadings. *European Journal of Mechanics - A/Solids* 23**,** 37-61.